

Hydrophobic–Hydrophilic Character of Hexamethyldisiloxane Films Polymerized by Atmospheric Pressure Plasma Jet

M. Bashir¹ · S. Bashir²

Received: 5 July 2014 / Accepted: 12 March 2015 / Published online: 31 March 2015
© Springer Science+Business Media New York 2015

Abstract This paper reports on polymerization of hexamethyldisiloxane (HMDSO) using an atmospheric pressure dielectric barrier discharge plasma jet. The aim of the study is to contribute to the knowledge of thin film deposition using a low cost technique of atmospheric pressure plasma. The monomer HMDSO was used as a precursor for polymerization. The discharge was powered using a laboratory made resonant power supply working with sinusoidal voltage signal at a frequency of 8 kHz. The coatings were characterized using Fourier transform infrared spectroscopy, atomic force microscopy, growth rates and surface free energy measurements. The hydrophobic nature of the films was found to be decreased with increasing the plasma power. Fourier transform infrared spectroscopy gave an indication of the dominated inorganic content of the surface at higher discharge. An average growth rate of 220 nm min⁻¹ was achieved at a monomer flow rate of 5 sccm and discharge power of 12.5 W. The films obtained using plasma jet were found to be stable in aqueous media and well adhered with substrate.

Keywords Atmospheric pressure plasma jet · Glass substrate · Polymerization · Surface properties

Introduction

Recently the development of atmospheric pressure plasma technology has gained much interest due to its wide range of applications [1, 2]. Different types of discharge sources have been developed and implemented for generating cold plasma at atmospheric pressure

✉ M. Bashir
m.bashir@comsats.edu.pk; dr.bashir77@gmail.com

¹ Department of Physics, COMSATS Institute of Information Technology, Islamabad, Pakistan

² Department of Physics and Applied Mathematics, Pakistan Institute of Engineering and Applied Sciences, P.O. Nilore, Islamabad, Pakistan

[3, 4]. Among these sources atmospheric pressure plasma jets based on the principle of corona discharge offer certain advantages for material processing. Corona discharges have a number of commercial and industrial applications due to their high concentration of radicals and ions [5]. However, the corona discharges generated with continuous wave signals are typically very low power which is unacceptable for many applications. The low power corona discharges are non-uniform and inefficient for material processing due to low density of the energetic species in plasma. The higher discharge power leads to the transition from corona to arc plasma. The unnecessary arcing can be avoided either by generating discharge with pulse-periodic mode or by introducing a dielectric barrier between two electrodes [6]. The latter has been adopted for this study. Dielectric barrier discharges (DBDs) are the most suitable sources for the generation of non thermal plasmas at atmospheric pressure due to their cold, robust and low frequency operation. Plasma deposition is an appropriate low temperature method used to deposit the functional coatings with required properties on a wide variety of substrates [7, 8]. The films are generally chemically inert due to high cross linking, ultra thin, pinholes free, thermally stable and have a good adhesion to the substrate. Technology based on plasma deposition is continuously developing and coating has a wide range of applications e.g., anticorrosion, protection, dielectrics for semiconductors and hydrophobic or hydrophilic for bio applications [8, 9].

Hexamethyldisiloxane (HMDSO) is a commonly used and preferred precursor for plasma polymerization as it is readily available low cost material and has high vapor pressure. Plasma polymerized hexamethyldisiloxane (PPHMDSO) films have a number applications such as biomedical, protective coatings, pharmaceutical packaging and microelectronics industries [10, 11]. There are several studies on plasma deposition of hexamethyldisiloxane using a low pressure vacuum system [12, 13]. However, low pressure coating systems are associated with practical limitations due to their low deposition rates, difficulty in integration and high cost of vacuum technology. As a consequence of these drawbacks the new technology based on atmospheric pressure deposition has gained much attention due to its flexibility in terms of low cost, ease of operation and integration for in-line processing. Compared to the deposition performed in vacuum, relatively few studies have been made that use the technique of atmospheric pressure plasma for polymerization of hexamethyldisiloxane [14–16], however, further work is required in order to explore the effect of parameters such as monomer concentration, gas flow rate and discharge power on properties of the deposited surface.

This paper presents the preparation and surface characterization of PPHMDSO films using an atmospheric pressure plasma jet. The effect of plasma processing parameters at atmospheric pressure on the surface of the polymerized films was studied using Fourier transform infrared spectroscopy (FTIR), atomic force microscopy (AFM) and growth rate analysis. The transition of the films from hydrophobic to hydrophilic was confirmed by measuring the contact angle of deionized (D.I.) water at the surface. The paper is structured as follows. The experimental methods and characterization techniques are described in “[Methods](#)” section. The results with discussion are presented in “[Results and Discussion](#)” section and the conclusions of this study are drawn in “[Conclusions](#)” section.

Methods

Deposition Setup

The experimental setup used for atmospheric pressure plasma deposition is sketched in Fig. 1a. A 99.9 % pure argon (Ar) gas was used for plasma generation and to carry the monomer vapors in reactor. A photograph of Ar plasma jet is shown in Fig. 1b. The monomer hexamethyldisiloxane with purity 99.5 % was sourced from Sigma Aldrich. The setup consists of two mass flow controllers to control the flow rate of Ar gas. One of the mass flow controllers having flow rate range of 0–30 sccm from Bronkhorst UK (F-201CV) and the other one with flow rate range of 80–1750 sccm from BOC UK (model: 846027) were used. A custom made glass bubbler was heated at 70 °C for vaporizing the monomer solution. A low flow rate of Ar gas (5–7.5 sccm) was passed through the bubbler and plasma deposition was achieved using vapors of HMDSO. The commercially available glass microslides were cut and used as a substrate for deposition. They were cleaned using methanol and deionized water. A circular area with an average diameter of 1.3 cm was deposited on the substrate.

Electrode Configuration for Plasma Jet

Figure 1 represents the schematic of an atmospheric pressure plasma jet. The arrangement is prepared in our laboratory and consists of a two concentric electrodes. The inner electrode is a steel wire of diameter 1.5 mm having one sharp end through which a high concentrated electric field emanate during jet plasma. The outer electrode is a circular aluminum sheet of thickness 0.5 mm and width 5 mm. The inner diameter of the glass tube is 5.5 mm and wall thickness is 1.25 mm which act as a DBD layer. The wire electrode is is

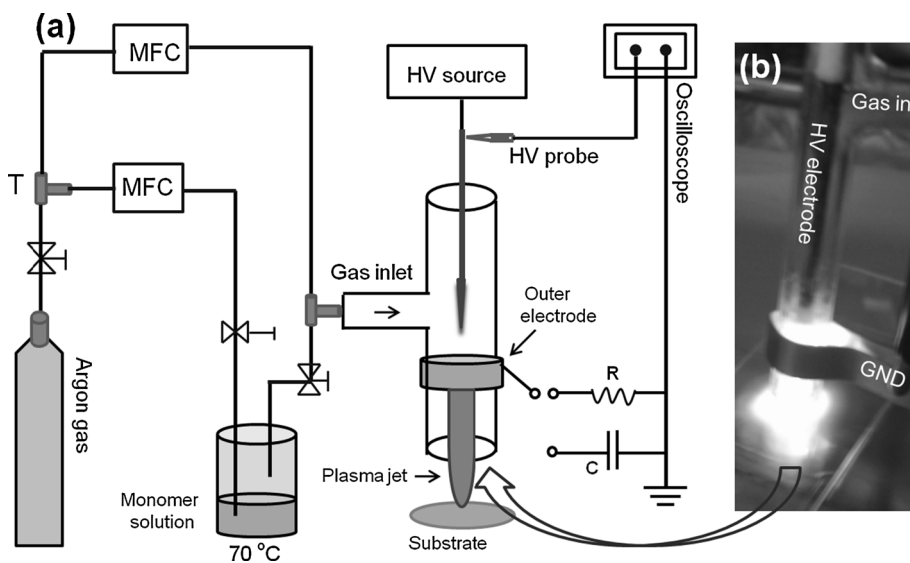


Fig. 1 a Schematic of experimental setup used for atmospheric pressure plasma deposition. b Photograph of the DBD plasma jet

inserted into another borosilicate glass capillary tube having inner diameter of 1.8 mm and wall thickness of 0.2 mm. This helps to avoid contamination from electrode erosion during plasma material processing. The wire electrode covered with capillary tube is fixed at the center of a glass tube and connected to the high voltage (HV) of plasma source while the outside aluminum electrode is grounded. When a high voltage electric field is applied the ionized gas from the plasma jet exits through the bottom end of the glass tube where it is directed onto a flat glass substrate. The tip of the high voltage electrode is adjusted very close to the upper end of round aluminum electrode. The distance between the lower end of aluminum electrode and bottom of glass tube is varied from 5 to 10 mm. The distance between the bottom end of glass tube and substrate is varied from 3 to 5 mm in order to optimize the jet formation according to the gas flow rate and discharge power.

Electrical Characterization of Plasma

Typically the electrical characterizations of atmospheric pressure plasma are performed by measuring the voltage and current along the plasma reactor. An oscilloscope (Picoscope ADC212) and a high voltage probe (Tektronix 1000:1) were used for measuring the voltage applied across the electrodes. A $50\ \Omega$ resistor was connected from the ground side of the reactor for measuring current and consequently plasma power. The current was measured in terms of voltage using the oscilloscope.

The charge versus voltage (Lissajous plot) method has been widely used for measuring the energy coupled to the discharge per cycle [17]. A capacitor with a known value of capacitance, 10 nF, was connected to the reactor from ground side. This known capacitance must be greater than the capacitance of the discharge channel otherwise according to the capacitive voltage division it will significantly change the voltage along the plasma electrodes. The voltage signals were recorded simultaneously along the plasma jet and the capacitor. The voltage and the capacitance of the capacitor gave the total charge flowing through the plasma during one cycle. The energy consumed per cycle of the voltage can be estimated by measuring the area of the Lissajous plot. The plasma power can be found by multiplying the energy consumed per cycle with the frequency of the applied voltage.

Fourier Transform Infrared Spectroscopy

The chemical composition of the plasma polymerized HMDSO films has been studied using Fourier transform infra red spectroscopy. The spectra were obtained by using FTIR spectrometer (Spectrum 100, Perkin Elmer USA) at a resolution of $4\ \text{cm}^{-1}$. The spectrometer was equipped with attenuated total reflectance (ATR) having a diamond crystal as an internal reflecting element. Thirty two scans were performed and then averaged for each sample. An error of $\pm 5\%$ is estimated for FTIR measurements.

Contact Angle Measurements

The wettability (hydrophilic or hydrophobic nature) of a solid surface can be examined easily by measuring the contact angle of a liquid drop with the solid surface. Since the technique is sensitive to the upper few atomic layers of the material (approximately 1 nm) it produces information concerning the energy available at the deposited surface which is not possible using spectroscopic measurements. The contact angles were measured using FTA 200 tensiometer. D.I. water was dropped onto the surface of the

sample with an average sessile volume of 7 μL and an error of $\pm 5\%$ is estimated for each measurement.

Atomic Force Microscopy and Film Thickness

The surface morphology of PPHMDSO films was observed using atomic force microscopy. The images of the surface were recorded using Digital Nanoscope 3100 by adopting the tapping mode of AFM. The scans were performed by selecting an area of $20\ \mu\text{m}^2$ at the surface of PPHMDSO.

The thickness of the plasma polymerized films was determined using AFM technique. The film was scratched using the tip of a sharp blade in order to make a step height to enable the thickness to be determined. The films with plasma jet were grown in a circular area of diameter around 1.3 cm. The film growth was non homogeneous along the radial direction of the circle. The thickness was found lower at the center and then gradually increased towards the outer edge. The film thickness was averaged over the values measured at three different points along the radial direction. There are no specific percentage error values given in each individual analysis, however, when the scanner for x, y and z was calibrated using a calibration standard the error in the z measurement was estimated to be less than $\pm 5\%$.

Growth Rate Measurements

As mentioned in “[Atomic Force Microscopy and Film Thickness](#)” section the deposition footprints showed non homogeneous film growth along the radial direction of the deposited circular area, therefore, we have analyzed the growth rates in μg per second instead of measuring deposition rates in terms of film thickness in μm per second. The mass of deposition was measured using a sensitive mass balance (PS-200, Fisher Scientific U.K.) with precision up to five significant figures. The substrates were cleaned by using ethanol and D.I. water. The cleaned substrates were blow dried with nitrogen gas and kept in an oven at $60\ ^\circ\text{C}$ for 30 minutes. They were weighed immediately before and after plasma deposition in order to measure the mass. An error of $\pm 10\%$ is added in the data which may come from mass balance reading plus due to the contamination from foreign particles on the surface during measurement.

Table 1 Deposition conditions for plasma polymerization of HMDSO

Processing parameters	Quantity
Ar gas flow rate (sccm)	800
Monomer flow rate (sccm)	5–7.5
Monomer temperature ($^\circ\text{C}$)	70
Pre-treatment time (min)	1
Deposition time (min)	2–10
Discharge power (W)	12.5–22.5

The discharge power is the output power of HV source applied across the jet reactor

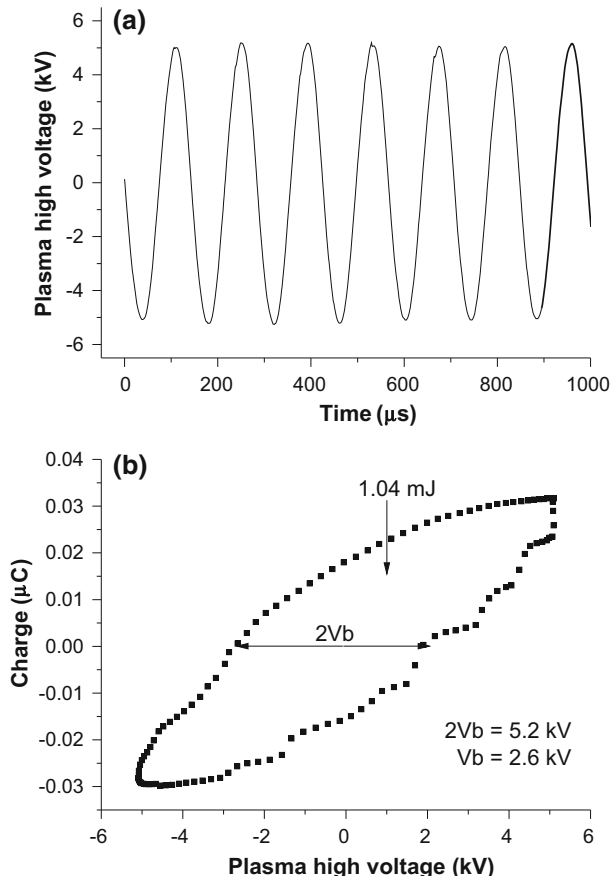
Results and Discussion

Plasma deposition was performed using a laboratory made DBD jet plasma configuration as described in “[Electrode Configuration for Plasma Jet](#)” section. The deposition conditions for plasma polymerization are summarized in Table 1. The distance between the bottom end of the glass tube and the substrate was fixed at 6 mm for the presented results. The monomer flow rate of 5 sccm, Ar gas flow rate of 800 sccm and a deposition time of 5 minutes were optimized and kept constant throughout the observation until otherwise stated. The optimal processing conditions for deposition were set by monitoring the stability of the films in aqueous media and its adhesion to the glass substrate.

Electrical Analysis of Discharge

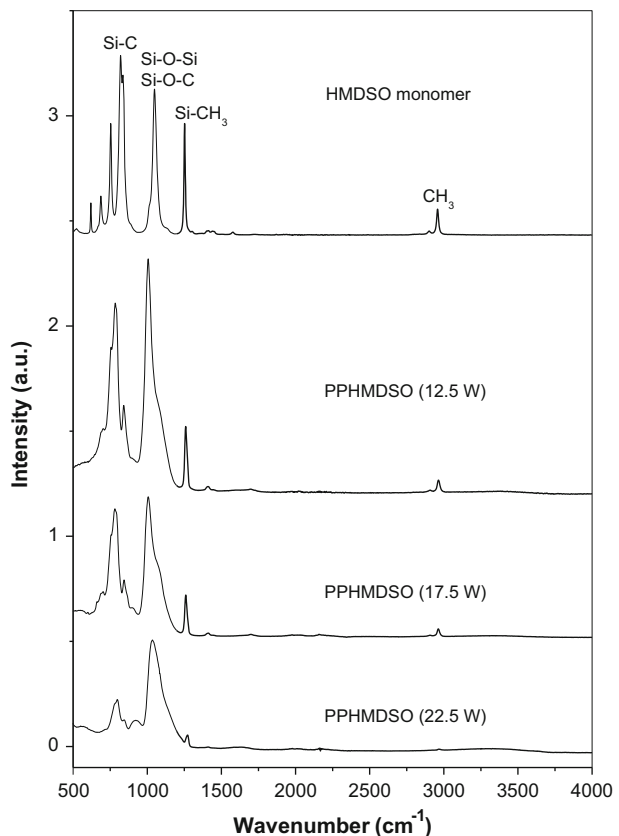
The high voltage signals applied to the plasma electrodes are shown in Fig. 2a. The voltage signals represent a sinusoidal wave with minimum distortions and have a peak to peak value of 10 kV. It is useful to monitor the output voltage signal during deposition as plasma instabilities may lead to a distorted signal. Figure 2a indicates that the plasma

Fig. 2 **a** Sinusoidal high voltage signals applied to the plasma electrodes and **b** Lissajous plot for DBD jet plasma at a peak applied voltage of 5 kV, switching frequency of 8 kHz. V_b represents the effective gas breakdown voltage and is equal to 2.6 kV



remained stable during deposition at a peak voltage of 5 kV and a frequency of 8 kHz. In 1943, Manley reported the electrical characterization of the ozonator discharge by using the charge transfer through DBD reactor versus applied voltage plot (Lissajous) [18]. After then this method has been extensively used to distinguish between different types of DBD discharges. Figure 2b shows the typical Lissajous plot for plasma jet. The Lissajous figure of the proposed jet plasma is not like a parallelogram which is a typical form for DBD plasma. It is similar to the almond shape as reported in several studies for DBD plasma [17, 19, 20]. Gibalov et al. [21] studied that the surface discharge continuously varies the shape of its volume discharge throughout each cycle and it leads to the change in the capacitance of the discharge during the cycle. This effect results in an almond-shaped Lissajous plot as represented in Fig. 2b. Moreover, the vertices of the plot are not as sharp as that of a low frequency DBD plasma it might indicate that the charging or discharging transition is not well defined in the DBD plasma upon the reversal of the electric field. The energy consumed per cycle of the discharge can be calculated from the area under the closed pattern of Lissajous plot and it is found to be 1.04 mJ. The power consumed per cycle for the discharge can be estimated by multiplying the calculated energy and the driving frequency which is 8 kHz. At an input power of 15 W the power consumed per cycle was found to be 8.3 W. It is noticeable that 55 % of the applied power (15 W) was utilized for plasma generation and the rest of 45 % was dissipated for charging and discharging the capacitive

Fig. 3 FTIR absorption spectra of monomer and plasma polymerized HMDSO deposited at different discharge powers. Films were prepared at monomer flow rate of 5 sccm and deposition time of 5 minutes



load. At a peak applied voltage of 5 kV, the effective gas breakdown voltage, V_b , calculated from Lissajous figure is 2.6 kV [22].

FTIR Analysis

FTIR spectra of HMDSO monomer and plasma polymerized films are shown in Fig. 3. The samples for FTIR analysis were prepared at a monomer flow rate of 5 sccm and deposition time of 5 minutes. A circular area of around 2.5 mm diameter can be scanned using attenuated total reflectance (ATR) accessory of FTIR machine. The position of the FTIR scans was at the center of the coated area. The comparison of the monomer spectrum with plasma polymers spectra shows that the monomer structure is more preserved for deposition performed at low power compared to those deposited at high power. The spectral peaks were identified with reference to previously published data [1, 23, 24]. The band assignments of FTIR spectra for HMDSO monomer and PPHMDSO are summarized in Table 2. The FTIR spectrum of monomer shows dominant absorption bands at 2958, 1252, 1048, 835, 820, and 754 cm^{-1} . The spectra of plasma polymerized HMDSO exhibits strong bands at 2965, 1260, 1006, 843 and 784 cm^{-1} . The absorption peaks at 2958–65 cm^{-1} can be attributed to CH_3 stretching vibrations. The peak at 1260 cm^{-1} can be assigned to the symmetric bending of Si-CH_3 . The absorption band at 843 cm^{-1} can be assigned to the Si-C rocking vibrations in the SiCH_3 groups. The peak at 784 cm^{-1} can also be attributed to the rocking vibration in SiCH_3 groups.

The films deposited at a low power (12.5 W) showed a low degree of monomer fragmentation. The relative intensity of the FTIR peaks related to the stretching vibration of CH_3 and Si-CH is gradually decreased on increasing plasma power as shown in Figs. 3 and 4. The intensities of different chemical peaks in FTIR spectra as a function of plasma power have been listed in Table 3. Figure 4 shows the ratio of the peaks attributed to SiOSi (hydrophilic) to CH_3 (hydrophobic). The increase in the ratio of SiOSi/CH_3 by increasing plasma power revealed a dominant hydrophilic character of the films at high power. Similar behavior of the films was observed by other researchers. For instance, Hayakawa et al. observed that the relative intensity of SiOSi peak was increased by increasing the plasma treatment time during deposition of hexamethyldisiloxane [8]. Twomey et al. [14] reported that hexamethyldisiloxane films exhibited more inorganic behavior upon increasing the plasma exposure. Morent et al. [25] obtained the similar results by increasing the flow rate of air in plasma during deposition of hexamethyldisiloxane.

It is noticeable that a significant amount of air can mix with plasma gas due to the deposition in an open environment via plasma jet. Most likely at higher power oxygen

Table 2 Band assignment for FTIR spectra of PPHMDSO

Materials	Position (cm^{-1})	Assignment
HMDSO monomer	2958	CH_3
	1252	Si-CH_3
	1048	Si-O-Si , Si-O-C
	835	Si-C
	820	Si-C
PPHMDSO	2965	CH_3
	1260	Si-CH_3
	1006	Si-O-Si , Si-O-C
	843	Si-C

Fig. 4 Intensities of CH₃, SiCH₃ peaks and ratio of SiOSi (hydrophilic) to CH₃ (hydrophobic) in FTIR spectra as a function of discharge powers

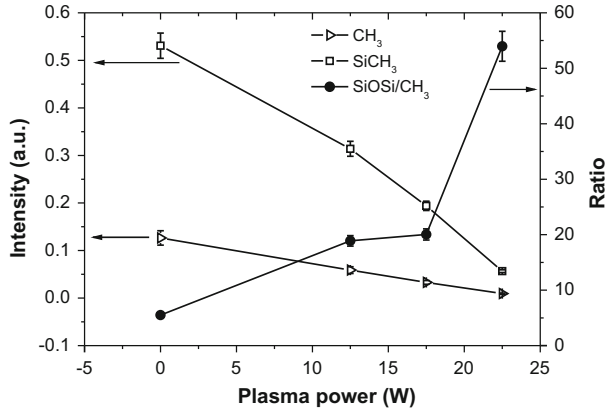


Table 3 Intensities of chemical peaks in FTIR spectra as a function of discharge power (estimated error $\pm 5\%$)

Material	Power (W)	Intensity (a.u.)				Ratio SiOSi/CH ₃
		CH ₃	SiCH ₃	SiOSi	SiC	
Monomer	–	0.1265	0.5309	0.6965	0.8541	5.51
Polymer	12.5	0.0588	0.3140	1.1107	0.8963	18.89
	17.5	0.0330	0.194	0.6613	0.6048	20.04
	22.5	0.0094	0.0566	0.5072	0.225	53.96

atoms or molecules can become active and they easily react with organic moieties of HMDSO molecules which increases the monomer fragmentation. Therefore a higher power discharge in the presence of oxygen can increase the consumption of C, CH and possibly Si radicals due to the formation of CO₂, H₂O and SiO₂ products resulting from the oxidation reactions [25, 26]. Lamendola et al. [26] reported that oxygen atoms or molecules can easily react with the organic moieties of HMDSO molecules and therefore promote the monomer fragmentation during deposition. Hence, most likely a higher power discharge in the presence of oxygen promotes the consumption of C, CH₃, Si radicals and the production of SiO₂ particles.

Surface Wettability and Energy Measurement

The surface free energy of the plasma polymerized films was calculated from the contact angle measurements of test liquids using the Owens–Wendt mathematical approach [27]. According to Owen’s method the surface free energy (γ_s) of a solid is equal to the sum of its dispersion (γ_s^d) and polar (γ_s^p) components, $\gamma_s = \gamma_s^d + \gamma_s^p$, and is given by the relation [28, 29]:

$$\gamma_{sL} = \gamma_s + \gamma_L - 2 \left[\sqrt{\gamma_s^d \gamma_L^d} + \sqrt{\gamma_s^p \gamma_L^p} \right], \quad (1)$$

where γ_{sL} is the free energy associated with the interface between the solid and the test liquid, γ_L is the surface free energy of the liquid, and γ_L^d and γ_L^p are the dispersion and polar components of the surface free energy respectively. The contact angle θ of a liquid drop at the surface of a solid substrate can be determined using Young's equation [30]:

$$\gamma_s - \gamma_{sL} = \gamma_L \cos \theta. \quad (2)$$

Using equation 1 to substitute for $\gamma_s - \gamma_{sL}$ leads to

$$(1 + \cos \theta) \gamma_L = 2 \sqrt{\gamma_s^d \gamma_L^d} + 2 \sqrt{\gamma_s^p \gamma_L^p}. \quad (3)$$

Equation 3 contains two unknowns, γ_s^d and γ_s^p . The values of these unknowns can be determined by measuring the contact angle at the surface of thin film using two different types of liquids (water and diiodomethane) with known values of γ_L^d and γ_L^p . Hence, the surface free energy can be calculated using equation 3 and the data available in Table 4. Figure 5 shows photographs of D.I. water droplets at the surface of plasma polymerized HMDSO. The contact angle (θ) of water droplets at the surfaces of plasma polymers was found to decrease by increasing the plasma power during deposition. The PPHMDSO surface deposited at lower power is hydrophobic with the highest value of contact angle $128^\circ \pm 6.4^\circ$ (Fig. 5b) and becomes hydrophilic (Fig. 5d) when deposited at higher power. The surface free energy of the films was calculated from the values of D.I. water contact angles measured from 9 different points at the surface of the films and then averaged for each of the samples. Figure 6 shows the variation in water contact angle, surface free energy, dispersive and polar components of surface energy as a function of discharge power. This signifies that the surface free energy of the plasma polymerized films is substantially high at the higher discharge power and vice versa. The results of the contact angle measurements corroborate with those obtained using FTIR spectroscopy. The increase in the surface free energy at higher power can be attributed to the increase of ratio SiOSi/CH₃ (Fig. 4) at higher power and hence, formation of hydrophilic SiO₂ particles. The coatings exhibited a higher dispersive component of the surface free energy at lower discharge power, however, the major contribution to the increase in surface free energy is from the polar component as the variation in the dispersive component with increasing power is relatively low (Fig. 6). Twomey et al. [14] reported the similar results for plasma polymerization of hexamethyldisiloxane. They stated that the surface free energy was increased by increasing the number of plasma exposures to the siloxane precursor. Moreover, Wenzel [31, 32] and Cassie [33] studied the effect of surface structure on

Table 4 Surface free energy, its dispersion and polar components for water and diiodomethane [29]

Liquid	γ_L (mJ m ⁻²)	γ_L^d (mJ m ⁻²)	γ_L^p (mJ m ⁻²)
Water	72.8	21.8	51.0
Diiodomethane	50.8	48.5	2.3

where γ_L , γ_L^d and γ_L^p represent the surface free energy, its dispersion and polar components of probe liquids respectively

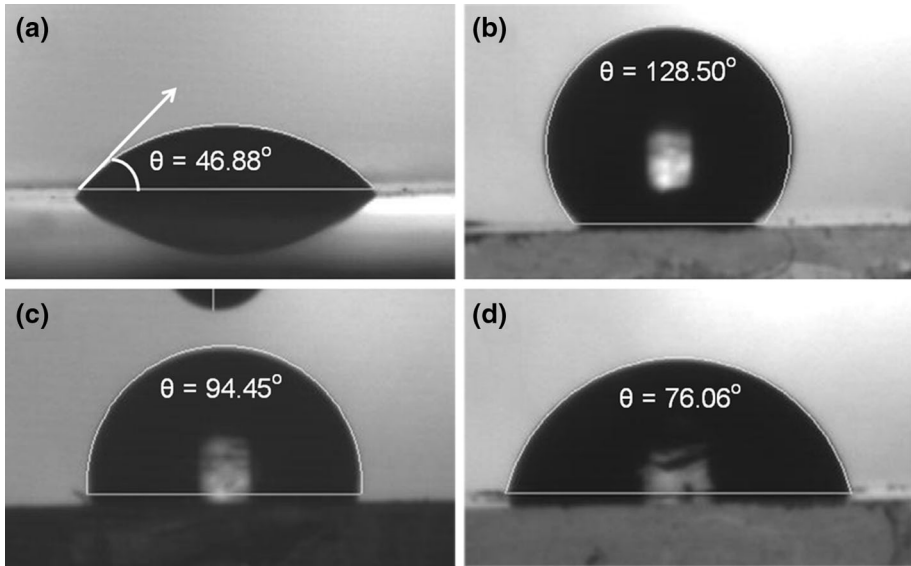
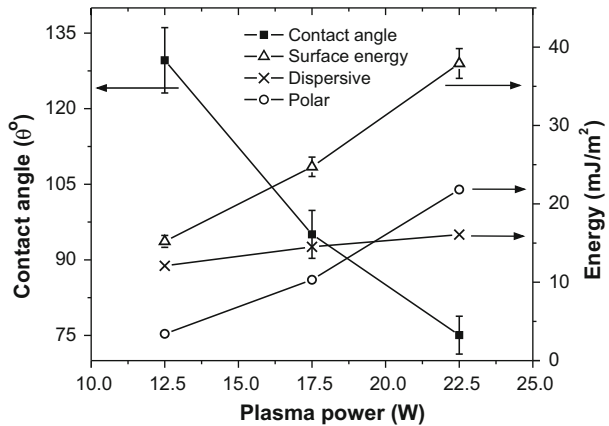


Fig. 5 D.I. water contact angle as a function of discharge power. **a** Untreated glass substrate, **b** PPHMDSO at power of 12.5 W, **c** PPHMDSO at power of 17.5 W and PPHMDSO at power of 22.5 W

Fig. 6 Deionized water contact angle, surface free energy, dispersive and polar components of surface energy as a function of discharge power



hydrophobic or hydrophilic nature of the surface. Both models predicted that hydrophobicity was increased by increasing the surface roughness. Since in this study the RMS value of the surface roughness decreases from 894 ± 44.7 to 439.9 ± 22 nm with an increase in discharge power from 12.5 to 22.5 W (see “Coating Morphology” section) this may enhance the surface wettability at higher plasma power. Table 5 enlists the values of water contact angles from previously published literature of plasma polymerized hexamethyldisiloxane. The results of contact angle measurements of the current study corroborate with those published previously. Hence, the films with promising characteristics (hydrophobic to hydrophilic) can be deposited by controlling the operating parameters of the jet plasma.

Table 5 A comparison of the wetting properties of HMDSO films with the properties of previously reported HMDSO films

Literature reports	Contact angle (°)	Processing conditions	Ref.
Morent et al.	102	Power: 12.6 W, atmospheric pressure	[25]
Lopez-Barrea et al.	100	Power: 50 W, atmospheric pressure	[35]
Levasseur et al.	136–121	Power: ~40 W, atmospheric pressure	[36]
Ji et al.	135	Power: 200 W, atmospheric pressure	[37]
Foest et al.	110–70	Power: 10–40 W, atmospheric pressure	[38]
Yeo et al.	90	Power: 60 W, pressure 0.5 Torr	[12]
Current study	128–76	Power: 12.5–22.5 W, atmospheric pressure	—

The films were stored in ambient environment for a period of 90 days and the ageing behavior was analyzed using contact angle measurements after storage. All of the plasma polymerized films showed ageing effects by decreasing the D.I. water contact angles after 90 days as listed in Table 6. The decrease in the water contact angle can be attributed to the formation of polar groups at the surface of polymer and surface oxidation via oxygen in the ambient air. The post-plasma surface oxidation is a well known phenomenon which takes place mainly because of reactions between the remaining radicals at the plasma treated surface and the atmospheric oxygen [34]. The sample deposited at lower plasma power (12.5 W) showed a significant decrease in the value of contact angle (128.5°–110.4°) during ageing process compared to those deposited at higher discharge power (22.5 W) which showed a slight decrease in contact angle (76.06°–73.1°) after 90 days.

Coating Morphology

Figure 7a–c show the AFM images for PPHMDSO surfaces deposited at discharge powers of 12.5, 17.5 and 22.5 W respectively. AFM analyses revealed that the surfaces deposited using plasma jet were continuous and free from pin holes or voids. The continuous surface without voids is most likely due to the deposition performed in the glow mode of the plasma jet (Fig. 1b). It has been already studied that the deposited films are continuous and relatively smoother when an atmospheric pressure glow discharge is used compared to those prepared in a filamentary mode of the discharge [39, 40]. The average value of surface roughness for glass substrate was found to be 0.415 ± 0.021 nm. The values of surface roughness for three places along with the radial direction of circular coating are listed in Table 7. Figure 7 shows the images of AFM scans performed at the central point of the coating. The RMS value of the surface roughness for films was decreased from 894 ± 44.7 to 439 ± 22 nm on increasing the discharge power. The decrease in the surface

Table 6 The surface ageing of PPHMDSO films after 90 days storage in ambient air (estimated error ± 5 %)

Plasma power (W)	Average contact angle (°)	
	Fresh	After 90 days
12.5	128.5	110.4
17.5	94.45	90.2
22.5	76.06	73.1

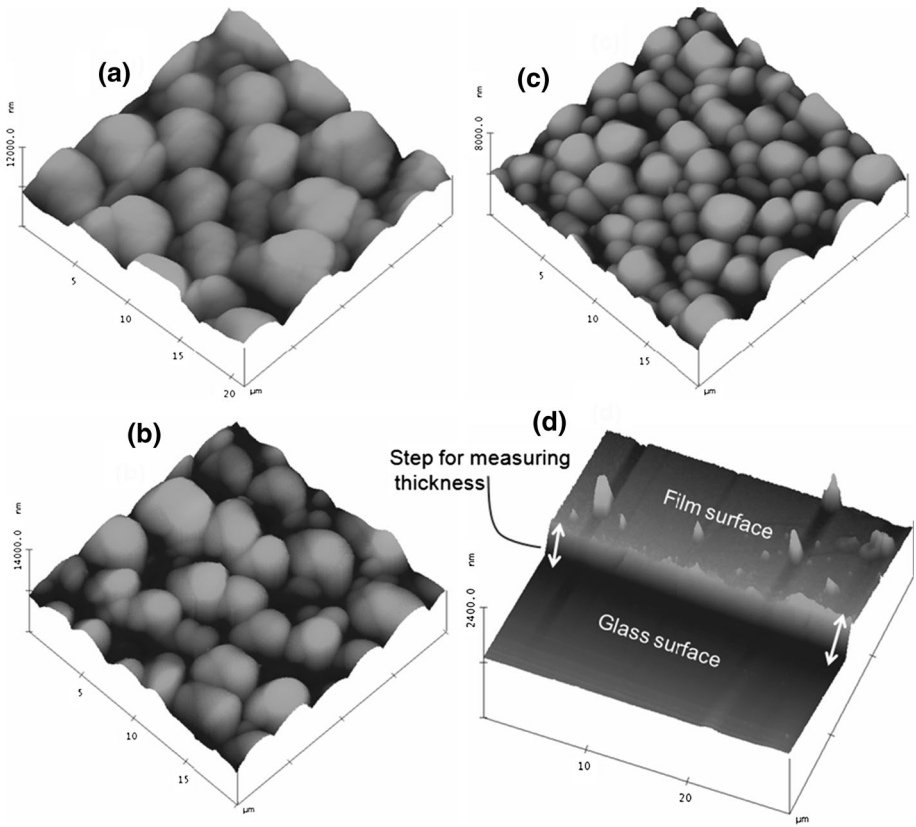


Fig. 7 Tapping mode AFM images of PPHMDSO films deposited at power of **a** 12.5 W with RMS roughness 894 ± 44.7 nm, **b** 17.5 W with RMS roughness 735.7 ± 36.8 nm and **c** 22.5 W with RMS roughness 439.9 ± 22 nm. **d** The image represents the step height for measuring thickness through AFM

Table 7 The surface roughness (estimated error $\pm 5\%$) measured using AFM for three different points along with the radial direction of PPHMDSO films

Power (W)	Central point (nm)	Mid point (nm)	End point(nm)
12.5	894	896	901
17.5	735.7	739.2	744
22.5	439.9	438.7	442.3

Mid point is at $r/2$ from the center

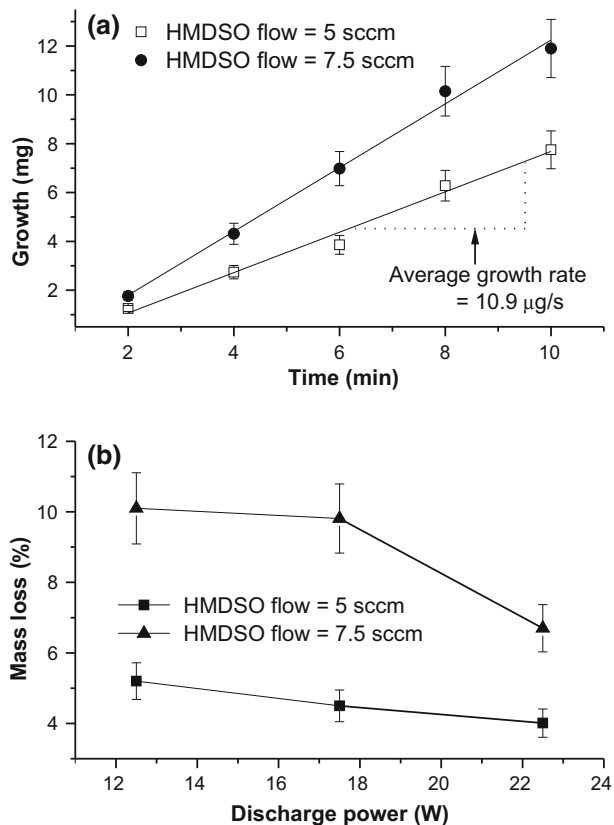
roughness at higher power can be attributed to the enhanced surface migration due to the plasma energetic particles at the polymer surface. Contrary to this at low power the energy of the particles at the surface is too small for significant migration. Furthermore, the AFM images show that the surface of the films consists of particles (grains) and the size of these grains is gradually decreased upon increasing the plasma power (Fig. 7a–c). In addition to the surface topography, AFM can also be used for measuring the thickness of the

PPHMDSO films. The samples were scratched and then were probed using AFM by scanning both the scratched and unscratched regions (Fig. 7d). The film growth was found non homogeneous along the radial direction of the circle. The thickness was averaged over the values measured at three different points along the radial direction. An average thickness of 662 ± 33 nm was found for the sample deposited at a discharge power of 12.5 W, monomer flow rate of 5 sccm and a treatment of 3 minutes. It gives an average deposition rate of 220 ± 11 nm min⁻¹ which is significantly higher than most of the previously reported growth rates for plasma jets. Han et al. [41] reported a growth rate of 170 nm min⁻¹ for their SiO₂ deposition using atmospheric pressure cold arc plasma jet. Zhu et al. [42] obtained a film growth rate of approximately 100 nm min⁻¹ for atmospheric pressure plasma deposition.

Growth Rate and Stability of the Film

The configuration of the plasma presented here is based on the principle of dielectric barrier corona discharge. As outlined earlier (“Introduction” section) corona discharges have a number of commercial and industrial applications due to their high concentration of radicals and ions. Therefore, DBD corona discharges can be efficiently used for film deposition with higher degree of cross linking and rapid growth rate. Figure 8a shows the

Fig. 8 **a** PPHMDSO growth as a function of deposition time and **b** mass loss in deionized water as a function of discharge power at two different monomer flow rates



deposition mass as a function of deposition time for monomer flow rates of 5 and 7.5 sccm. A linear relationship was observed for polymerization time of 10 minutes. An average growth rate of $10.9 \pm 1.09 \mu\text{g s}^{-1}$ for monomer flow rate of 5 sccm and $17.85 \pm 1.8 \mu\text{g s}^{-1}$ for monomer flow rate of 7.5 sccm was calculated from the slope of linear fit as shown in Fig. 8a. The procedure for mass loss analysis has been reported in detail in our previous studies [3]. In brief the coated samples were submersed in D.I. water immediately after deposition and slowly stirred for half an hour. The analyses were performed by measuring the weights before and after submersion. Figure 8b shows the percentage mass loss of the films which was obtained by washing them in D.I. water as a function of plasma power. The mass loss was decreased by increasing the discharge power. It can be attributed to the increase in the number of cross-linking of polymer chains due to the dissociation of monomer molecules at enhanced electric field and consequently the formation of higher molecular weight material. The films deposited at a monomer flow rate of 7.5 sccm showed a relatively higher mass loss in D.I. compared to those obtained at a monomer flow rate of 5 sccm (Fig. 8b). According to Yasuda [43], the value of the composite parameter, W/FM, decreases by increasing the flow rate (F) at a constant discharge power (W) and a molecular weight (M) of the monomer. This relation shows that the energy available per unit molecule of the gas decreases by increasing the monomer flow rate at constant plasma power which reduces the polymer cross-linking due to a lower molecular fragmentation. Thus, it is necessary to select the optimal parameters such as power and flow rate in order to deposit the film having good cross linking and the required chemical functionality.

Conclusions

The plasma polymerized HMDSO films were obtained using atmospheric pressure DBD plasma jet under different discharge conditions of monomer flow rate and applied power. The effect of discharge power on the surface of the deposited films was investigated using contact angle measurements, FTIR spectroscopy and AFM technique. The FTIR spectra indicated that a low power discharge produced hydrophobic PPHMDSO films with maximum retention of chemical groups of original monomer structure. The intensity of the FTIR peaks which contribute to the film hydrophobicity was significantly decreased on increasing the discharge power. The D.I. water contact angles measured at the surface were gradually decreased (128° – 76°) on increasing the plasma power (12.5–22.5 W). An average growth rate of $10.9 \pm 1.09 \mu\text{g s}^{-1}$ in terms of mass and $220 \pm 11 \text{ nm min}^{-1}$ in terms of the film thickness was obtained for a monomer flow rate of 5 sccm and a discharge power of 12.5 W. The mass loss analysis showed that the films were found to be stable in D.I. water by optimizing the processing parameters. Hence, the films with promising characteristics can be obtained by changing the plasma conditions.

Acknowledgments M.B. would like to acknowledge the Higher Education Commission of Pakistan for financial support through its IPFP program.

References

1. Fang J, Chen H, Yu X (2001) Studies on plasma polymerization of hexamethyldisiloxane in the presence of different carrier gases. *J Appl Polym Sci* 80:1434–1438

2. Asandulesa M, Topala I, Pohoata V, Dumitrascu N (2000) Influence of operational parameters on plasma polymerization process at atmospheric pressure. *J Appl Phys* 108:093310–093315
3. Bashir M, Rees JM, Zimmerman WB (2013) Plasma polymerization in a microcapillary using an atmospheric pressure dielectric barrier discharge. *Surf Coat Technol* 234:82–91
4. Bradley JW, Oh J-S, Olanbaji OT, Hale C, Mariani R, Kontis K (2011) Schlieren photography of the outflow from a plasma jet. *IEEE T Plasma Sci* 39:2312–2313
5. Goldman M, Goldman A, Sigmund RS (1985) The corona discharge, its properties and specific uses. *Pure Appl Chem* 57:1353–1362
6. Bashir M, Bashir S, Rees JM, Zimmerman WB (2014) Surface coating of bonded PDMS microchannels by atmospheric pressure microplasma. *Plasma Process Polym* 11:279–288
7. Luo HL, Sheng J, Wan YZ (2007) Plasma polymerization of styrene with carbon dioxide under glow discharge conditions. *Appl Surf Sci* 253:5203–5207
8. Hayakawa T, Yoshinari M, Nemoto K (2004) Characterization and protein-adsorption behavior of deposited organic thin film onto titanium by plasma polymerization with hexamethyldisiloxane. *Biomaterials* 25:119–127
9. Yasuda H (1984) Plasma polymerization for protective coatings and membranes. *J Membr Sci* 18:273–284
10. Muguruma H, Hiratsuka A, Karube I (2000) Thin-film glucose biosensor based on plasma-polymerized film: simple design for mass production. *Anal Chem* 72:2671–2675
11. Homma T, Yamaguchi M, Kutsuzama Y, Otstuka N (1999) Electrical stability of polyimide siloxane films for interlayer dielectrics in multilevel interconnections. *Thin Solid Films* 340:237–241
12. Yeo S, Kwon T, Choi C, Park H, Hyun JW, Jung D (2006) The patterned hydrophilic surfaces of glass slides to be applicable for the construction of protein chips. *Curr Appl Phys* 6:267–270
13. Wei J, Igarashi T, Okumori N, Igarashi T, Maetani T, Liu B, Yoshinari M (2009) Influence of surface wettability on competitive protein adsorption and initial attachment of osteoblasts. *Biomed Mater* 4:045002–045008
14. Twomey B, Rahman M, Byrne G, Hynes A, OHare L-A, O'Neill L, Dowling D (2008) Effect of plasma exposure on the chemistry and morphology of aerosol-assisted, plasma-deposited coatings. *Plasma Process Polym* 5:737–744
15. Raballand V, Benedikt J, von Keudell A (2008) Deposition of carbon-free silicon dioxide from pure hexamethyldisiloxane using an atmospheric microplasma jet. *Appl Phys Lett* 92:091502–091504
16. Massines F, Gherardi N, Fornelli A, Martin S (2005) Atmospheric pressure plasma deposition of thin films by Townsend dielectric barrier discharge. *Surf Coat Tech* 200:1855–1861
17. Kriegseis J, Moller B, Grundmann S, Tropea C (2011) Capacitance and power consumption quantification of dielectric barrier discharge (DBD) plasma actuators. *J Electrostat* 69:302–312
18. Manley TC (1943) The electric characteristics of the ozonator discharge. *J Electrochem Soc* 84:83–96
19. Bashir M, Rees JM, Bashir S, Zimmerman WB (2014) Characterization of atmospheric pressure microplasma produced from argon and a mixture of argon-ethylenediamine. *Phys Lett A* 378:2395–2405
20. Nagao I, Nishida M, Yukimura K, Kambara S, Maruyama T (2002) NOx removal using nitrogen gas activated by dielectric barrier discharge at atmospheric pressure. *Vacuum* 65:481–487
21. Gibalov VI, Pietsch GJ (2000) The development of dielectric barrier discharges in gas gaps and on surfaces. *J Phys D Appl Phys* 33(20):2618
22. Reddy EL, Biju VM, Subrahmanyam Ch (2012) Production of hydrogen from hydrogen sulfide assisted by dielectric barrier discharge. *Int J Hydrogen Energy* 37:2204–2209
23. Kale KH, Palaskar S (2010) Atmospheric pressure plasma polymerization of hexamethyldisiloxane for imparting water repellency to cotton fabric. *Text Res J* 81:608–620
24. Lee SH, Lee DC (1998) Preparation and characterization of thin films by plasma polymerization of hexamethyldisiloxane. *Thin Solid Films* 325:83–86
25. Morent R, Geyter ND, Vlierbergh SV, Dubrue P, Leys C, Schacht E (2009) Organic-inorganic behaviour of HMDSO films plasma-polymerized at atmospheric pressure. *Surf Coat Tech* 203:1366–1372
26. Lamendola R, d' Agostino R, Fracassi F (1997) Thin film deposition from hexamethyldisiloxane fed glow discharges. *Plasma Polym* 2:147–164
27. Owens DK, Wendt RC (1969) Estimation of the surface free energy of polymers. *J Appl Polym Sci* 13:1741–1747
28. Pelagade SM, Singh NL, Rane RS, Mukherjee S, Deshpande UP, Ganesan V, Shripathi T (2012) Investigation of surface free energy for PTFE polymer by bipolar argon plasma treatment. *JSEMAT* 2:132–136
29. Zenkiewicz M (2001) Wettability and surface free energy of corona-treated biaxially-oriented polypropylene. *J Adhes Sci Technol* 15(14):1769–1785

30. Berthier J, Silberzan P (2006) *Microfluidics for biotechnology*, 1st edn. Artech house, London
31. Wenzel RN (1949) Surface roughness and contact angle. *J Phys Chem* 53:1466–1467
32. Wenzel RN (1936) Resistance of solid surfaces to wetting by water. *Ind Eng Chem* 28:988–994
33. Cassie DAB, Baxter S (1944) Wettability of porous surfaces. *Trans Faraday Soc* 40:546–551
34. Siow KS, Britcher L, Kumar S, Griesser HJ (2006) Plasma methods for the generation of chemically reactive surfaces for biomolecule immobilization and cell colonization—a review. *Plasma Process Polym* 3:392–418
35. Lopez-Barrea JA, Pimentel-Tinoco OG, Olayo-Valles R, Morales-Corona J, Olayo R (2014) Water permeability of quarry stone superficially modified by plasma polymerization of hexamethyldisiloxane at atmospheric pressure. *J Coat Tech Res* 11:661–664
36. Levasseur O, Stafford L, Gherardi N, Naude N, Blanchard V, Blanchet P, Riedl B, Sarkissian A (2012) Deposition of hydrophobic functional groups on wood surfaces using atmospheric-pressure dielectric barrier discharge in helium-hexamethyldisiloxane gas mixtures. *Plasma Process Polym* 9:1168–1175
37. Ji Y-Y, Kim S-S, Kwon O-P, Lee S-H (2009) Easy fabrication of large-size superhydrophobic surfaces by atmospheric pressure plasma polymerization with non-polar aromatic hydrocarbon in an in-line process. *Appl Surf Sci* 255:4575–4578
38. Foest R, Kindel E, Lange H, Ohl A, Stieber M, Weltmann K-D (2007) RF capillary jet—a tool for localized surface treatment. *Contrib Plasma Phys* 47:119–128
39. Trunec D, Navratil Z, Stahel P, Zajickova L, Bursikova V, Cech J (2004) Deposition of thin organo-silicon polymer films in atmospheric pressure glow discharge. *J Phys D Appl Phys* 37:2112–2120
40. Sira M, Trunec D, Stahel P, Bursikova V, Navratil Z (2008) Surface modification of polycarbonate in homogeneous atmospheric pressure discharge. *J Phys D Appl Phys* 41:015205–015212
41. Han MH, Noh JH, Lee TJ, Choi JH, Park KW, Hwang HS, Song KM, Baik HK (2008) High-rate SiO₂ deposition by oxygen cold arc plasma jet at atmospheric pressure. *Plasma Process Polym* 5:861–866
42. Zhu X, Arefi-Khonsari F, Petit-Etienne C, Tatoulian M (2005) Open air deposition of SiO₂ films by an atmospheric pressure line-shaped plasma. *Plasma Process Polym* 2:407–413
43. Yasuda H (1985) *Plasma polymerization*. Academic Press, New York